

Saturation of the free carrier absorption in ZnTe crystals

S. A. Ku,¹ C. M. Tu,¹ W.-C. Chu,¹ C. W. Luo,^{1,*} K. H. Wu,¹ A. Yabushita,¹ C. C. Chi,²
and T. Kobayashi,^{1,3}

¹Department of Electrophysics, National Chiao Tung University, Hsinchu, Taiwan

²Department of Physics, National Tsing Hua University, Hsinchu, Taiwan

³Advanced Ultrafast Laser Research Center, and Department of Engineering Science, Faculty of Informatics and Engineering, The University of Electro-Communications, Chofugaoka 1-5-1, Chofu, Tokyo 182-8585 Japan

*cwluo@mail.nctu.edu.tw

Abstract: This study systematically investigates the influence of free carriers on the generation of THz in ZnTe crystals, over a wide range of pumping fluences. As the pumping fluence is increased ($< 6.36 \text{ mJ/cm}^2$), the concentration of free carriers gradually increases and the THz output power is saturated, as clearly demonstrated by the time delay in the THz temporal waveforms, the changes in the THz spectral weight and the red-shift in the PL spectra. For high pumping fluences ($> 6.36 \text{ mJ/cm}^2$), spectacularly, there is a significant quadratic increase in the THz output power when the pumping fluence is increased, as well as at low pumping fluences of $< 0.58 \text{ mJ/cm}^2$, because of the saturation of free carriers.

©2013 Optical Society of America

OCIS codes: (190.7110) Ultrafast nonlinear optics; (260.3090) Infrared, far.

References and links

1. B. Ferguson and X.-C. Zhang, "Materials for terahertz science and technology," *Nat. Mater.* **1**(1), 26–33 (2002).
2. E. G. Sun, W. Ji, and X.-C. Zhang, "Two-photon absorption induced saturation of THz radiation in ZnTe," *Proceedings of the Conference on Lasers Electro-Optics*, OSA, 2000, 479–480.
3. V. Y. Gaivoronsky, M. M. Nazarov, D. A. Sapozhnikov, Y. V. Shepelyavyi, S. A. Shkel'nyuk, A. P. Shkurinov, and A. V. Shuvaev, "Competition between linear and nonlinear processes during generation of pulsed terahertz radiation in a ZnTe crystal," *Quantum Electron.* **35**(5), 407–414 (2005).
4. M. C. Hoffmann, K.-L. Yeh, J. Hebling, and K. A. Nelson, "Efficient terahertz generation by optical rectification at 1035 nm," *Opt. Express* **15**(18), 11706–11713 (2007).
5. S. M. Harrel, R. L. Milot, J. M. Schleicher, and C. A. Schmuttenmaer, "Influence of free-carrier absorption on terahertz generation from ZnTe (110)," *J. Appl. Phys.* **107**(3), 033526 (2010).
6. S. Vidal, J. Degert, M. Tondusson, J. Oberlé, and E. Freysz, "Impact of dispersion, free carriers, and two-photon absorption on the generation of intense terahertz pulses in ZnTe crystals," *Appl. Phys. Lett.* **98**(19), 191103 (2011).
7. T. Löffler, T. Hahn, M. Thomson, F. Jacob, and H. G. Roskos, "Large-area electro-optic ZnTe terahertz emitters," *Opt. Express* **13**(14), 5353–5362 (2005).
8. F. Blanchard, L. Razzari, H.-C. Bandulet, G. Sharma, R. Morandotti, J.-C. Kieffer, T. Ozaki, M. Reid, H. F. Tiedje, H. K. Haugen, and F. A. Hegmann, "Generation of 1.5 microJ single-cycle terahertz pulses by optical rectification from a large aperture ZnTe crystal," *Opt. Express* **15**(20), 13212–13220 (2007).
9. A. A. Said, M. Sheik-Bahae, D. J. Hagan, T. H. Wei, J. Wang, J. Young, and E. W. Van Stryland, "Determination of bound-electronic and free-carrier nonlinearities in ZnSe, GaAs, CdTe, and ZnTe," *J. Opt. Soc. Am. B* **9**(3), 405–414 (1992).
10. M. Schall and P. U. Jepsen, "Above-band gap two-photon absorption and its influence on ultrafast carrier dynamics in ZnTe and CdTe," *Appl. Phys. Lett.* **80**(25), 4771–4773 (2002).
11. C.-M. Tu, S. A. Ku, W.-C. Chu, C. W. Luo, J.-C. Chen, and C.-C. Chi, "Pulsed terahertz radiation due to coherent phonon-polariton excitation in $<110>$ ZnTe Crystal," *J. Appl. Phys.* **112**(9), 093110 (2012).
12. H. Wang, K. S. Wong, B. A. Foreman, Z. Y. Yang, and G. K. L. Wong, "One-and two-photon-excited time-resolved photoluminescence investigations of bulk and surface recombination dynamics in ZnSe," *J. Appl. Phys.* **83**(9), 4773–4776 (1998).
13. J. D. Ye, S. L. Gu, S. M. Zhu, S. M. Liu, Y. D. Zheng, R. Zhang, and Y. Shi, "Fermi-level band filling and band-gap renormalization in Ga-doped ZnO," *Appl. Phys. Lett.* **86**(19), 192111 (2005).
14. J. Liu, G. Kaur, and X.-C. Zhang, "Photoluminescence quenching dynamics in cadmium telluride and gallium arsenide induced by ultrashort terahertz pulse," *Appl. Phys. Lett.* **97**(11), 111103 (2010).
15. M. C. Hoffmann and D. Turchinovich, "Semiconductor saturable absorbers for ultrafast terahertz signals," *Appl. Phys. Lett.* **96**(15), 151110 (2010).

16. M. Nagai, M. Jewariya, Y. Ichikawa, H. Ohtake, T. Sugiura, Y. Uehara, and K. Tanaka, "Broadband and high power terahertz pulse generation beyond excitation bandwidth limitation via $\chi^{(2)}$ cascaded processes in LiNbO₃," *Opt. Express* **17**(14), 11543–11549 (2009).
 17. D. Turchinovich and M. C. Hoffmann, "Self-phase modulation of a single-cycle terahertz pulse by nonlinear free-carrier response in a semiconductor," *Phys. Rev. B* **85**(20), 201304 (2012).
 18. N. Kamaraju, S. Kumar, E. Freysz, and A. K. Sood, "Influence of two photon absorption induced free carriers on coherent polariton and phonon generation in ZnTe crystals," *J. Appl. Phys.* **107**(10), 103102 (2010).
-

1. Introduction

Terahertz (THz) science has seen significant developments over past decades and has a large number of applications in plasma physics, astronomy, medical imaging, biology and communication [1]. It is certainly important for the development of bright and broadband THz sources. Of the various techniques used, optical rectification in ZnTe crystals is mostly used for the generation of THz waves. However, the saturation of THz output power generated from ZnTe crystals limits the development of intense THz sources [2]. There have been many studies of the saturation mechanism of THz output power [3–6]. Some researchers focus on the study of large-area THz emitters, which avoid the creation of too many carriers and reduce the THz output power [7, 8]. Recently, it has been proved that the saturated THz conversion efficiency of ZnTe crystals mainly depends on free carrier absorption, rather than the pumping power, which is attenuated by two-photon absorption [5, 6]. These studies used ultrafast laser amplifiers with high pulse energy. The red shift in the THz spectra of ZnTe crystals and other nonlinear effects due to high pumping fluences (below the damage threshold) has not been explained, because of the lack of wide range and finely tuned pumping fluences.

This study uses a high-power Ti:sapphire laser with fine tuning of the fluences as a pumping source. To the authors' best knowledge, this is the first time that these issues have been studied over a wide range of pumping fluences. In order to determine the relationship between free carriers and THz generation in ZnTe crystals, the dependence of the THz temporal waveforms (spectra) and the photoluminescence (PL) radiated from ZnTe crystals on the pumping fluences is measured simultaneously. The effect of band gap renormalization, carrier saturation and PL quenching on THz generation are also determined.

2. Experiments

2.1 THz generation in ZnTe crystals

In these experiments, a long cavity Ti:sapphire oscillator (Femtsource scientific XL300, Femtolaser) with a central wavelength of 800 nm, a repetition rate of 5.2 MHz and a pulse duration of 70 fs was used for THz wave generation and detection. The pump beam, with a spot diameter of 46 μm , was focused on a 1-mm-thick (110) ZnTe crystal with the resistivity of 100 Ω/cm . A teflon filter was used to block the fundamental light whereas THz wave transmitting. The transmitted THz wave was collimated and focused on another 0.5-mm-thick (110) ZnTe, which detected the THz wave by free space electro-optical (EO) sampling through a pair of off-axis parabolic mirrors. All of the experiments were performed in a dry nitrogen-purged box. While the power of probing pulses for the EO sampling was kept constant, the pumping power used in this study was varied from 10 mW to 800 mW by a neutral density (ND) filter, which corresponds to 0.12~9.26 mJ/cm^2 . The dispersion due to a ND filter was compensated by a compressor inside the laser system. For convenience of analysis, the experimental results were classified into three regimes: a region of relatively low pumping fluences (0.12~0.58 mJ/cm^2), a region of medium pumping fluences (0.58~6.36 mJ/cm^2) and a region of relatively high pumping fluences (6.36~9.26 mJ/cm^2).

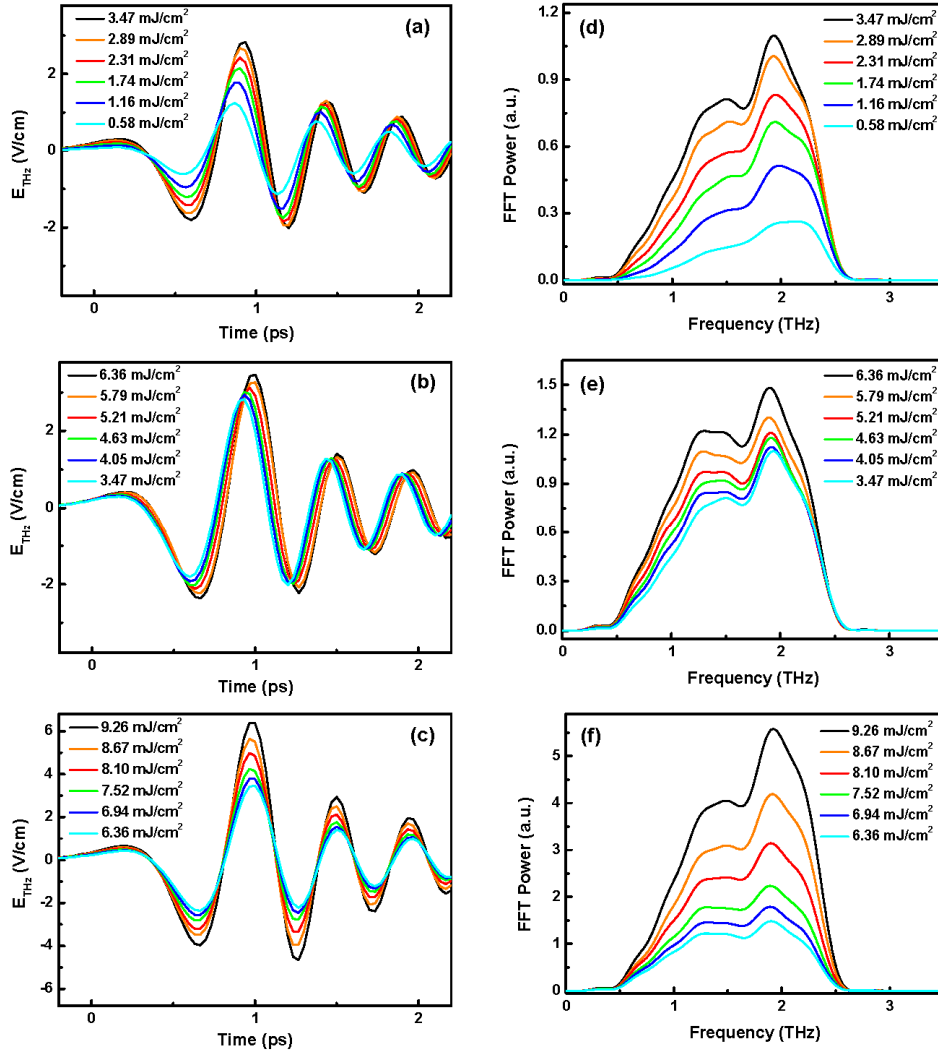


Fig. 1. (a)-(c) Temporal waveforms of the THz pulses generated by optical rectification in a ZnTe crystal at various pumping fluences. (d)-(f) The FFT spectra of the THz waveforms in (a)-(c).

The THz temporal waveforms at various pumping fluences in the range from 0.58 mJ/cm^2 to 9.26 mJ/cm^2 are shown in Figs. 1(a)-1(c). As the pumping fluence increases, a delay (shift in time) in the THz waveforms is clearly observed [as shown in Figs. 1(a) and 1(b)]. However, this type of time delay in THz temporal waveforms does not continuously increase in the high pumping fluence regime [as shown in Fig. 1(c)]. The delay in the THz temporal waveforms occurs because of a change in the refractive index, which is described by the relationship: $\Delta t = \Delta n \cdot d / c$, where d is the crystal thickness, c is speed of light, Δn is the change in the refractive index in the THz or the optical (fundamental) regimes. For pumping fluences of 4.63 mJ/cm^2 and 0.58 mJ/cm^2 , the time difference, Δt , between the temporal waveforms is approximately 80 fs, which corresponds to a value of $\Delta n = 2.4 \times 10^{-2}$. The possible reasons for the delay in the high pumping fluence regime are as follows: (1) High pumping fluences in the crystals may change the refractive index in the optical range (the optical Kerr effect). However, according to Ref [9], the change in the refractive index in the optical range is too small ($\Delta n \sim 10^{-4}$) to explain the delay in the THz temporal waveforms (In

this study, $\Delta n = 2.4 \times 10^{-2}$). (2) Photo-excited free carriers change the optical parameters, e.g. the refractive index of ZnTe crystals in the THz range [10]. This suggests that the free carriers created by two-photon absorption causes a change in the refractive index of ZnTe crystals in the THz range. Surprisingly, the THz temporal waveforms are not shifted more at high pumping fluences ($> 6.36 \text{ mJ/cm}^2$) as shown in Fig. 1(c). This demonstrates that the refractive index of ZnTe crystals does not change further as the pumping fluence is increased. In other words, the free carriers saturate in the ZnTe crystals and the refractive index in the THz range remains unchanged at pumping fluences of more than 6.36 mJ/cm^2 . This carrier saturation phenomenon is further verified by the photoluminescence results, which are discussed later.

The THz power spectra [Figs. 1(d)-1(f)] were obtained by fast Fourier transform of the THz temporal waveforms in Figs. 1(a)-1(c). The THz spectra generated from ZnTe crystals have two parts: a low-frequency part at $\sim 1.2 \text{ THz}$ and a high-frequency part at $\sim 1.9 \text{ THz}$ (the phase-matched frequency). The low-frequency part leads the high-frequency part in time, because of the normal dispersion material (ZnTe) through which the radiated THz waves pass. Therefore, the components of the THz temporal waveforms can be described as follows: the main THz pulse corresponds to the low-frequency part of the THz power spectra and the following oscillation corresponds to the high-frequency part (the phase-matching frequency) [11]. In the regime, $0.58 \sim 6.36 \text{ mJ/cm}^2$, the increase in rate of the high-frequency part in THz spectra is smaller than that for the low-frequency part as the pumping fluence increases, which demonstrates that the growth rate for the last oscillations is smaller than that of the THz main pulse. At pumping fluences greater than 6.36 mJ/cm^2 , the spectra do not change as the pumping fluence is increased. This coincides with an absence of any shift in the THz temporal waveforms [Fig. 1(c)]. Consequently, the THz spectra and the temporal waveforms as a function of pumping fluences are highly correlated with the concentration of free carriers in the ZnTe crystals. The change in the refractive index, Δn , for 800 nm or THz are is too small to cause a change in the emitted THz spectra and the temporal waveforms. Instead, free carriers in a ZnTe crystal cause absorption and affect the emitted THz waveforms and spectra.

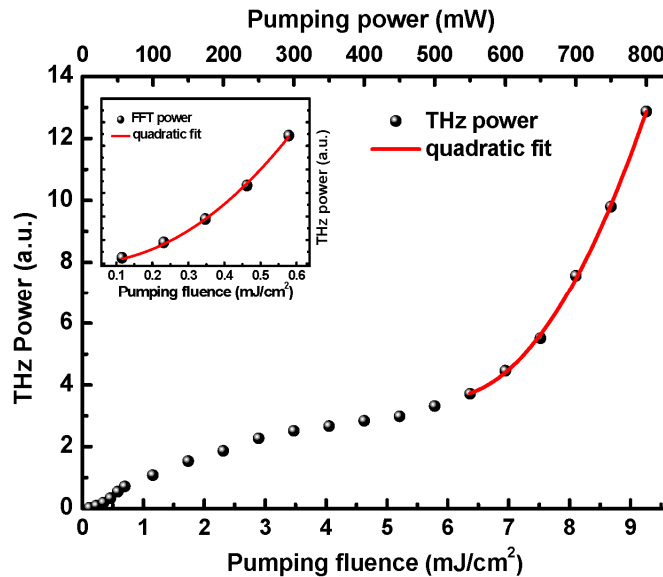


Fig. 2. The dependence of THz output power on pumping fluences in a 1-mm ZnTe crystal. The solid line presents the quadratic fit. Inset: an enlargement of the low pumping fluence regime.

The quadratic relationship between THz output power and the pumping fluences of less than 0.58 mJ/cm^2 is shown in the inset of Fig. 2. As the pumping fluence increases, the increase in the THz output power does not obey a quadratic relationship when the pumping

fluence is larger than 0.58 mJ/cm^2 , which is consistent with the results of Hoffmann et al. [4]. This is because the free carriers in the ZnTe crystals, whose concentration increases when the pumping fluence is increased, attenuate the THz output power. Moreover, in the regime of $3.47\text{--}6.36 \text{ mJ/cm}^2$, the THz output power remains almost constant, even if the pumping fluence is increased. Interestingly, in the extremely high pumping fluence regime of above 6.36 mJ/cm^2 , the THz output power is no longer reduced by saturation of the free carriers and there is a quadratic relationship between the pumping fluences and the THz output power, as shown by the solid line in Fig. 2. Meanwhile, the saturation of the free carriers does not cause further change in the refractive index of the ZnTe crystals and there is no further shift in the THz temporal waveforms.

2.2 Photoluminescence radiated from ZnTe crystals

After pumping, the free carriers in ZnTe crystals move from the conduction band to the valence band and emit a Yellow-green photoluminescence (PL) as shown in the inset of Fig. 3. In this study, the PL in the front of the ZnTe was measured using a fiber-coupled spectrometer (Ocean Optics USB4000) with a short pass filter. The two-photon absorption excites free carriers within the entire ZnTe crystal and the radiated PL must be transmitted and reabsorbed by the ZnTe crystal. The two-photon excited PL spectra represent the band gap edge of the excited ZnTe crystals. At a pumping fluence of 0.58 mJ/cm^2 , the PL is too weak to be isolated from the background noise. When the pumping fluence is increased, a relative red shift in the peak of PL spectra is observed, as shown in Fig. 3(a), which indicates the band gap renormalization (BGR) effect that is caused by the screening effect from extra carriers. The repulsion between free carriers results in a smaller band gap, so the relative amount of photo-excited free carriers can be estimated from the shift in the peak of the PL spectra. The red shift in the PL spectrum is usually described by the empirical relationship [12, 13]:

$$\Delta E_{\text{PL}} = E_g - E_0 = -K \cdot n^{1/3} \quad (1)$$

where K is the BGR coefficient and n is the concentration of the free carriers. The $n^{1/3}$ dependence of ΔE_{PL} resembles the prevailing exchange contribution of electron-electron interaction. In the pumping regime of $1.16\text{--}6.36 \text{ mJ/cm}^2$, the monotonic red shift in the PL spectra [Fig. 3(a)] indicates that the concentration of the free carriers in the ZnTe crystals rises as the pumping fluence increases. This result confirms that a greater number of free carriers results in a greater time delay in the THz temporal waveforms (see Fig. 1) and a greater attenuation of the THz output power (see Fig. 2). At pumping fluences greater than 6.36 mJ/cm^2 , however, the position of the peak in the PL spectra remains almost constant. In other words, the concentration of the free carriers no longer increases in the high pumping fluence regime, from 6.36 to 9.26 mJ/cm^2 , which provides direct evidence of saturation of the free carrier absorption effect in ZnTe crystals.

By integrating the PL spectra at various wavelengths, the intensity of PL signal can be calculated. This reveals how many carriers move from the conduction band to the valence band. The dependence of the intensity of the PL signal on pumping-fluence is shown in Fig. 3(b). At pumping fluences of less than 6.36 mJ/cm^2 , the intensity of the PL signal gradually increases, when the pumping fluence is increased. This indicates an increase in the number of free carriers, which causes a change in the refractive index in the THz range. At pumping fluences greater than 6.36 mJ/cm^2 , all of the results including the time delay in the THz temporal waveforms, the quadratic increase in the THz output power and the red shift in the PL spectra suggest that the concentration of free carriers remains constant. However, the intensity of the PL signal decreases in this regime. This implies that some free carriers transit back to the ground state by emitting luminescence decreases. On the other hand, intense THz waves may induce carrier recombination through non-radiative interaction, which is termed “The THz quenching effect” [14].

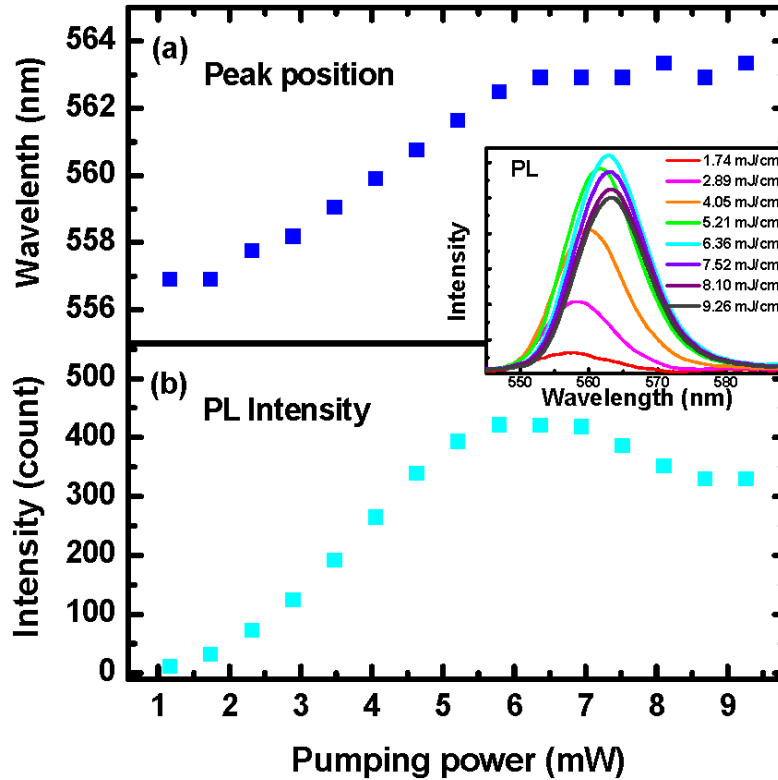


Fig. 3. (a) The position of the peak in the PL spectra for a ZnTe crystal as a function of pumping fluences. (b) The PL intensity as an integral of the emission spectra.

3. Discussion

In order to understand the mechanism for the reduction in THz output power, the time-evolution attenuation within a single THz temporal waveform at various pumping fluences was quantitatively analyzed. The time-dependent attenuation fraction for a single THz temporal waveform [e.g. Figure 4(a)] is given by:

$$A(t) = \frac{E_{THz}(P_1, t)}{E_{THz}(P_0, t) \times \frac{P_1}{P_0}} \quad (2)$$

where E_{THz} is the THz temporal waveform, P_0 is a pumping fluence of 0.58 mJ/cm^2 (without attenuation by free carriers) and P_1 is a higher pumping fluence (with attenuation by free carriers). In Fig. 4(b), the symbols show the time-dependent attenuation fraction at a pumping fluence of 4.63 mJ/cm^2 (the divergent points before 0.25 ps are artificial from calculation), wherein the solid line is a guide for the eyes. The THz attenuation fraction decreases within several hundreds of femtoseconds and then remains constant. The reasons for this time-dependent THz attenuation shown in Fig. 4(b) are as follows: (1) THz attenuated by free carrier absorption is associated with the number of free carriers and their mobility, (2) a rapid increase in THz attenuation requires that the free carriers take several hundreds of femtoseconds to achieve carrier thermalization in the conduction band (from higher energy levels to low energy levels in conduction band), after two-photon absorption and (3) during the flat portion of THz attenuation, the free carriers require more than 40 ps to relax from the conduction band to the valence band. Because the amount of free carriers does not change

during the 2nd and 3rd cycles of the THz temporal waveform, the attenuation by free carriers is almost the same within this period. As a consequence, a THz wave with a shorter pulse duration (generated by thinner ZnTe crystals) is less attenuated by free carrier absorption at the same pumping fluence.

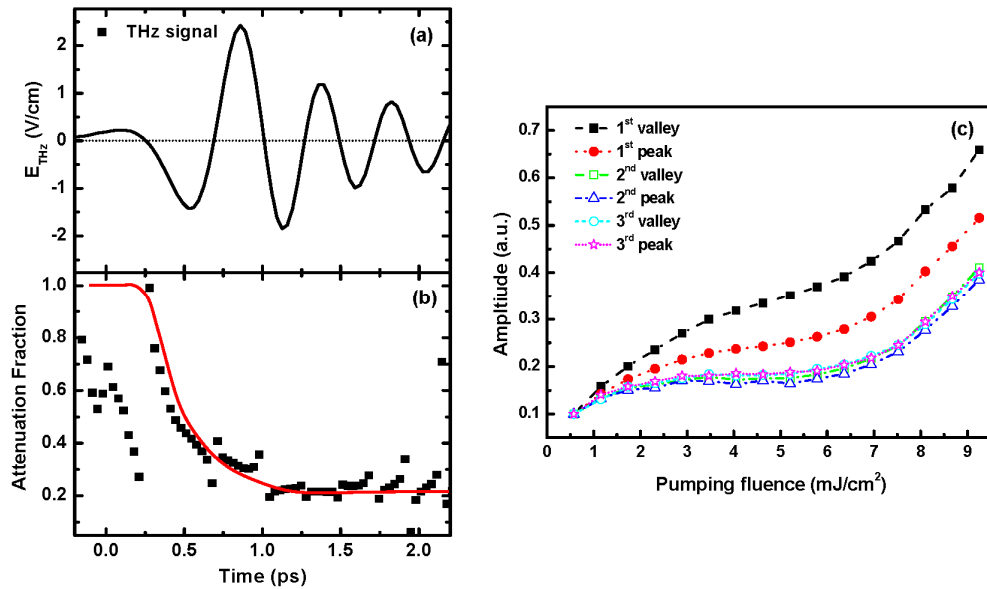


Fig. 4. (a) The THz temporal waveform radiated from a ZnTe crystal at a pumping fluence of $4.63 \text{ mJ}/\text{cm}^2$. (b) The attenuation fraction of a THz temporal waveform in (a) compared with that at a low pumping fluence of $0.58 \text{ mJ}/\text{cm}^2$. The solid line is a guide to the eyes. (c) The amplitude of the peaks and valleys in THz temporal waveforms as a function of the pumping fluences, which is normalized to a value for the pumping fluence of $0.58 \text{ mJ}/\text{cm}^2$.

The peak (valley) amplitude of the THz temporal waveforms was also calculated as a function of the pumping fluences. In principle, the peak (valley) amplitude of the THz temporal waveforms should increase linearly, without free carrier absorption. Actually, they do not increase linearly, because of free carrier absorption, similarly to previous results. The increase in amplitude of the first cycle of the THz temporal waveforms is more rapid than that in the following cycles, as the pumping fluence increases. Namely, the attenuation in the first cycle of the THz temporal waveforms is smaller than that for the following cycles. The large THz attenuation within the first cycle ($\sim 300 \text{ fs}$) verifies the result in Fig. 4(b). The subsequent cycles of the THz temporal waveforms demonstrate similar increases for various pumping fluences, which is consistent with the flat THz attenuation after 1 ps as shown in Fig. 4(b).

For the high pumping fluences ($> 6.36 \text{ mJ}/\text{cm}^2$), the saturation of free carriers in ZnTe crystals is clearly demonstrated by the analysis of the THz waveform and the PL spectra. This saturation phenomenon of the free carriers results in characteristics that are significant to THz generation in ZnTe crystals at high pumping fluences: (1) no further time delay is observed in the THz temporal waveforms because there is no further change in the refractive index of the ZnTe crystals, (2) the THz output power increases quadratically when the pumping fluence is increased and (3) there is no shift in the position of the peak in the PL spectra. At high pumping fluences greater than $6.36 \text{ mJ}/\text{cm}^2$, thus, the THz electric field strength linearly raises as increasing pumping fluences [Fig. 4(c)] due to the saturation of the free carrier absorption. This saturation of free carrier absorption effect has two possibilities. One is the saturation of free carrier concentration. The other one is the reduction of free carrier absorption with smaller carrier mobility or larger effective mass of hot carriers by high THz field strength [15]. For intense THz, the smaller carrier mobility or larger effective mass will cause the change of the refractive index inside crystals and deform the THz waveforms in the

time domain. Also, the spectra of optical pumping pulses and THz pulses after passing through ZnTe crystals gradually shift to lower frequency and become broader in high frequency side as increasing pumping fluences, respectively [16]. However, we did not observe the broadening of THz spectra in Fig. 1 and the red shift of optical spectra for pumping pulses, especially for high pumping fluence regime ($> 6.36 \text{ mJ/cm}^2$). In this study, the strongest peak field strength inside the crystal is around 6.3 V/cm as shown in Fig. 1 (THz pulse energy $\sim 1.84 \text{ pJ}$), which is corresponding to the THz fluence of around $0.03 \text{ } \mu\text{J/cm}^2$. The THz field strength and intensity in this study are much smaller than the values (several hundred kV/cm) studied in Ref [17].

Moreover, the nonlinear plasma response in the crystals would raise the effective mass of hot electrons and modify the curvature of conduction band to lead a relatively change in the bandwidth of PL spectra. Based on our experimental results of the PL spectra in high pumping fluence regime ($> 6.36 \text{ mJ/cm}^2$), however, we did not observe any changes in the bandwidth and the shift in peak position as shown in the inset of Fig. 3. Only the PL intensity shrinks as increasing the pumping fluences, which is consistent with the results of Ref [14]. It means no more changes for the band structure of ZnTe crystals (such as band gap renormalization). On the other hand, we did not observe the time shift in the THz temporal waveforms as shown in Fig. 1(c), which is caused by the intense THz field (several hundred kV/cm) in Ref [17]. Consequently, we conclude that the quadratic increasing of THz output power is due to the saturation of free carrier, and the reason of PL intensity decreasing observed at high pumping fluences of greater than 6.36 mJ/cm^2 in this study would be mainly dominated by the "PL quenching effect". Based on these results, we propose some methods for the reduction of THz attenuation, e.g. shortening the lifetime of carriers (by using another probe light to induce stimulated emission in ZnTe crystals), or changing the optical properties of the ZnTe crystals (by using crystals with different purity [18]).

4. Conclusion

The characteristics of the THz and PL signals radiated from ZnTe crystals over a wide range of pumping fluences are systematically studied in this paper. In the low pumping fluence regime ($0.58 \text{ mJ/cm}^2 \sim 6.36 \text{ mJ/cm}^2$), the concentration of free carriers in the ZnTe crystals increases as the pumping fluence is increased, which results in a band gap renormalization (i.e. a red shift in the PL spectra) in the ZnTe crystals. These free carriers in the ZnTe crystals not only affect the refractive index in the THz range, but also cause a time-dependent attenuation of the THz temporal waveforms.

In the high pumping fluence regime (above 6.36 mJ/cm^2), the saturation of free carriers in the ZnTe crystal is clearly demonstrated by the unchanged position of the peak in the PL spectra. Therefore, the THz temporal waveforms are not subject to further delay because of the unchanged refractive index in the THz range. Moreover, there is a quadratic increase in the THz output power as the pumping fluence is increased, which is also seen in the results for very low pumping fluences ($< 0.58 \text{ mJ/cm}^2$). These results demonstrate that there is a potential for intense THz generation in semiconducting nonlinear materials.

Acknowledgment

This work was supported by the National Science Council of Taiwan, R.O.C. under grant: NSC101-2112-M-009-016-MY2, and by the Grant MOE ATU Program at NCTU.